Published in final edited form as:

Science. 2021 May 07; 372(6542): . doi:10.1126/science.abf8424.

Environmental robustness of the global yeast genetic interaction network

Michael Costanzo[1,*], **Jing Hou**[1,*], **Vincent Messier**[1,*], **Justin Nelson**[2,3,*], **Mahfuzur Rahman**[2,3,*], **Benjamin VanderSluis**[2], **Wen Wang**[2], **Carles Pons**[4], **Catherine Ross**[1], **Matej Ušaj**[1], **Bryan-Joseph San Luis**[1], **Emira Shuteriqi**[1], **Elizabeth N. Koch**[2], **Patrick Aloy**[4,5], **Chad L. Myers**[2,3,#], **Charles Boone**[1,6,7,#], **Brenda Andrews**[1,6,#]

[1.]The Donnelly Centre, University of Toronto, 160 College St., Toronto ON, Canada M5S 3E1

[2.]Department of Computer Science & Engineering, University of Minnesota-Twin Cities, 200 Union St., Minneapolis MN, U.S.A. 55455

[3.]Program in Biomedical Informatics and Computational Biology, University of Minnesota- Twin Cities, 200 Union St., Minneapolis MN, U.S.A. 55455

[4.]Institute for Research in Biomedicine (IRB Barcelona), The Barcelona Institute for Science and Technology, Barcelona Spain

[5.]Institució Catalana de Recerca I Estudis Avaçats (ICREA), Barcelona Spain

[6.]Department of Molecular Genetics, University of Toronto, 160 College St., Toronto ON, Canada M5S 3E1

[7.]RIKEN Center for Sustainable Resource Science, Wako, Saitama, Japan

Abstract

Phenotypes associated with genetic variants can be altered by interactions with other genetic variants (GxG), with the environment (GxE), or both (GxGxE). Yeast genetic interactions have been mapped on a global scale, but the environmental influence on the plasticity of genetic networks has not been examined systematically. To assess environmental rewiring of genetic networks, we examined 14 diverse conditions and scored 30,000 functionally representative yeast gene pairs for dynamic, differential interactions. Different conditions revealed novel differential interactions, which often uncovered new functional connections between distantly related gene pairs. However, the majority of observed genetic interactions remained unchanged in different conditions, suggesting that the global yeast genetic interaction network is robust to environmental perturbation and captures the fundamental functional architecture of a eukaryotic cell.

[#]To whom correspondence should be addressed. cmyers@umn.edu, charlie.boone@utoronto.ca, brenda.andrews@utoronto.ca.
[*]These authors contributed equally to this work

Author contributions: M.C., C.L.M., C.B., and B.A. conceived and coordinated the project. V.M, B.S.L. and E.S. performed genetic interaction experiments. J.H., V.M., J.N., M.R., B.V.S., W.W., C.P., C.R., M.U., E.N.K. and P.A. analyzed the data. M.C., J.H., C.L.M., C.B. and B.A. prepared the manuscript.

Competing interests: The authors declare no competing interests.

Data and material availability: All Data Files associated with this study are available for download from the DRYAD Digital Repository (doi:10.5061/dryad.3r2280gfd) or from https://boonelab.ccbr.utoronto.ca/condition_sga/

Graphical Abstract

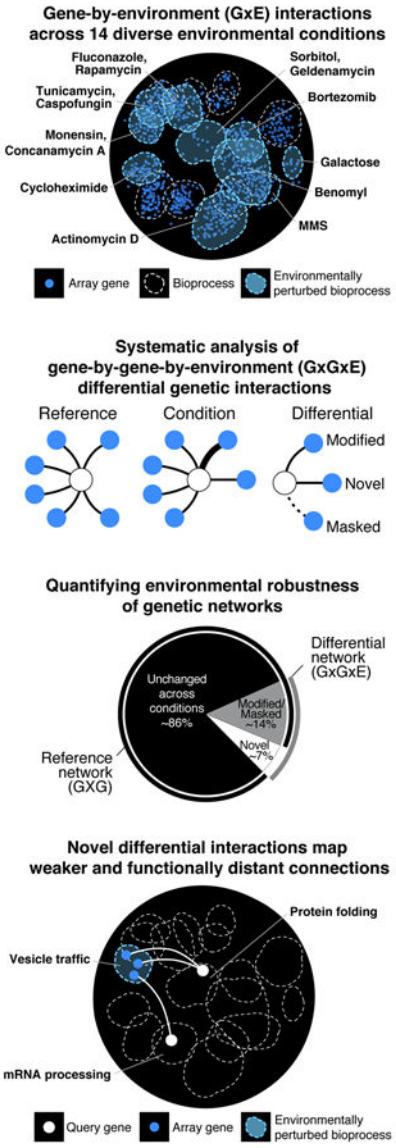

Systematic analysis of environmental impact on the global yeast genetic interaction network. Mapping gene-by-environment (GxE) interactions and gene-by-gene-by-environment (GxGxE) differential interactions reveals the environmental robustness of the global yeast genetic interaction network, highlighting new and distant functional connections associated with novel differential interactions.

Abstract

Introduction: Genetic interactions are identified when variants in different genes combine to generate an unusual phenotype compared to the expected combined effect of the corresponding individual variants. For example, a synthetic lethal genetic interaction occurs when two mutations, neither of which is lethal on their own, combine to generate a lethal double mutant phenotype.

While there are millions of possible gene-gene combinations for any eukaryotic cell, only a rare subset of gene pairs will display a genetic interaction. Digenic, or gene-by-gene (GxG), interactions appear to underlie key aspects of biology, including the relationship between genotype and phenotype. Environmental conditions can modulate the phenotype associated with genetic variants, giving rise to gene-by-environment (GxE) interactions, when a single variant phenotype is modified, or gene-by-gene-by-environment (GxGxE) interactions when a genetic interaction is changed.

Rationale: A global genetic interaction network has been mapped for the budding yeast *Saccharomyces cerevisiae*, identifying thousands of connections that often occur between functionally related genes. Because the global genetic network was mapped in a specific reference condition, the potential for different environmental conditions to rewire the network remains unclear. Automated yeast genetics, combined with knowledge of a reference map, enables quantification of the extent to which new environmental conditions either modulate known genetic interactions or generate novel genetic interactions to influence the genetic landscape of a cell.

Results—We tested ~4,000 yeast single mutants for GxE interactions across 14 diverse environments, including an alternative carbon source, osmotic and genotoxic stress, and treatment with 11 bioactive compounds targeting distinct yeast bioprocesses. To quantify GxGxE interactions, we constructed ~30,000 different double mutants, involving genes annotated to all major yeast bioprocesses, and we scored them for genetic interactions. The plasticity of the network is revealed by differential genetic interactions, which occur when a genetic interaction observed in a particular condition deviates from that scored in the control reference network.

Although ~10,000 differential interactions were discovered across all 14 conditions, we observed ~3-fold fewer differential interactions per condition compared to genetic interactions in the reference condition, indicating that GxGxE interactions are rare relative to GxG interactions. On average, a single environmental perturbation modulated ~14% of the reference genetic interactions and revealed a smaller subset of ~7% novel differential interactions. While GxG genetic interactions tend to connect pairs of genes that share a close functional relationship, novel differential GxGxE interactions mediate weaker connections between gene pairs with diverse roles.

Conclusion—Although different environments have the potential to reveal novel interactions and uncover new but weaker functional connections between genes, the vast majority of genetic interactions remained unchanged in different conditions, suggesting that the global yeast genetic interaction network is largely robust to environmental perturbation.

Extrapolation of our findings suggest that a systematic survey of genetic interactions in a sensibly chosen model cell may be sufficient to map a reference genetic network that encompasses a core set of widely expressed genes, providing a basic scaffold for the genetic wiring of a human cell.

Because the yeast genetic network is robust to environmental perturbation, we suspect it will be robust to genetic background changes, which further suggests that a systematic survey of genetic interactions in a sensibly chosen model cell should be sufficient to map a reference genetic network that encompasses a core set of widely expressed genes, providing a basic scaffold for the genetic wiring of a human cell.

Genetic interactions are identified when two or more different gene variants combine to cause an unusual phenotype that deviates from a model based on the combined effects of the corresponding single variant phenotypes (1). Digenic or gene-by-gene (GxG) interactions appear to underlie diverse and fundamental aspects of biology, including the relationship between genotype and phenotype, the evolution of sexual reproduction, and speciation (2–6). The phenotype associated with genetic variants can also be modulated by environmental factors, including growth conditions, age, cell type, or microbe exposure, giving rise to gene-by-environment (GxE) interactions, or gene-by-gene-by-environment (GxGxE) interactions if a genetic interaction is modified. Eukaryotic genomes contain thousands of different genes, millions of possible genetic interactions and function in many environmental contexts, meaning that our ability to explore the extent to which genetic interactions contribute to trait heritability is a major combinatorial and statistical challenge (3).

Efforts to address this challenge have involved the systematic mapping of genetic interactions in accessible model systems, primarily the budding yeast, *Saccharomyces cerevisiae.* Large-scale application of an automated genetic approach, Synthetic Genetic Array (SGA) analysis, enabled the majority of all possible gene pairs to be tested for negative and positive genetic interactions (7, 8). A negative genetic interaction corresponds to a synthetic lethal or sick interaction when a double mutant shows a fitness defect greater than the expected effect of the combined single mutant fitness phenotypes. Conversely, a positive genetic interaction is scored in a double mutant that grows better than expected (9). Genetic suppression represents an extreme type of positive interaction, where the double mutant fitness phenotype is greater than that of the least fit single mutant (10). The resultant global digenic interaction network comprises ~350,000 positive and ~550,000 negative interactions, which tend to connect pairs of functionally related genes (11, 12). Genes encoding members of the same biological pathway or protein complex often share similar patterns or profiles of negative and positive genetic interactions, and a global network clusters genes with similar genetic interaction profiles together into a hierarchy of organized modules, corresponding to protein complexes/pathways, biological processes and cellular compartments, revealing the functional architecture of a eukaryotic cell (Fig. 1A)(11, 12).

The reference yeast genetic network was mapped in a single genetic background in a specific reference condition. The phenotypes of both single and double mutant cells can be modulated by the environment, which leads to GxE and more complex GxGxE interactions. For example, subsets of functionally biased yeast genes have been surveyed in response to several different environmental conditions, and condition-specific genetic interactions have been identified (13–18). However, given the focus so far on specific bioprocesses, such as DNA repair, the plasticity of genetic networks across a broad array of environmental conditions remains unclear. Here, we systematically assess GxE and GxGxE effects in the context of the structure and topology of the global yeast genetic interaction network. This powerful model system allows us to assess the extent to which the environment modulates genetic interactions to influence the overall genetic landscape of a cell and provides important insights into the utility of genetic network reference maps.

Single mutant fitness and gene-environment interactions

Quantitative analysis of digenic interactions depends on accurate assessment of single and double mutant phenotypes (19). Therefore, to accurately measure the effect of environment on the yeast genetic network, a baseline of quantitative measurements of condition-specific effects on single mutant fitness (GxE interactions) is required. To identify GxE interactions in the context of an SGA screen, we subjected an array of single mutants to SGA analysis using a neutral (control) “query” locus and assessed colony size following growth in different conditions. We examined 14 diverse conditions, including an alternative carbon source, osmotic stress, genotoxic stress and 11 bioactive compounds that target distinct yeast biological processes within the global genetic interaction profile similarity network (Fig. 1A,B). Relative fitness measurements were obtained for 3,704 viable deletion mutant strains and 782 temperature-sensitive (TS) alleles, corresponding to 553 essential genes, both in the reference SGA condition and in each of the 14 diverse conditions (Data File 1)(20–23).

To identify GxE interactions from our single mutant fitness measurements, we calculated a differential fitness score for each mutant by measuring the difference between mutant fitness in the reference condition versus each of the 14 conditions (fig. S1A)(23). More than half of all the genes that we examined (59%) were associated with a significant differential single mutant fitness defect ($P < 0.05$, differential fitness score < -0.08)(see Method Summary and (23) for details) in at least one condition (fig. S1B). The union of all genes that displayed fitness defects in each condition revealed that 6 to 8 conditions identified the majority of unique genes associated with condition-specific growth defects (fig. S1C). Additional conditions captured relatively few new genes, perhaps because different conditions can lead to a similar stress response (24). Thus, our set of 14 conditions affects a wide range of functionally diverse genes and should be useful for exploring how different environments impact overall structure and topology of the global genetic interaction network.

The total number of strains with detectable differential fitness defects in a single condition ranged from ~250 (4.5%) to ~1,200 (22%), with the largest number of condition-specific fitness defects observed in the presence of Benomyl, a microtubule depolymerizing agent (fig. S1D). Stronger negative differential fitness scores were associated with genes encoding known targets of compounds (fig. S1A). More generally, genes with differential fitness defects in a particular growth condition were often involved in a specific function perturbed by the corresponding growth condition (fig. S2, Data File 2)(20). For example, in Benomyl, numerous genes involved in mitosis or DNA replication and repair were enriched for differential fitness defects (Fig. 1C, Data File 2)(20). A number of genes involved in mRNA processing also displayed fitness defects in Benomyl, which may reflect that genes encoding α-tubulin, *TUB1* and *TUB3*, are among the relatively few yeast genes with introns (Fig. 1C, Data File 2)(20, 25). In contrast, the differential fitness defects in Monensin, an intracellular traffic inhibitor (26), were most enriched among genes involved in vesicle trafficking, glycosylation, and cell wall biosynthesis (Fig. 1D, Data File 2)(20).

Some mutants (1,083) had positive differential fitness scores, indicating better growth relative to a wild-type strain in a particular condition compared to the corresponding mutant growth relative to wild-type in the reference condition (fig. S1A, B, D). For

example, although all strains, including wild type, grew more slowly in the presence of the proteasome inhibitor, Bortezomib, strains carrying TS alleles of essential genes were enriched among the set of mutant strains that showed positive differential fitness scores in this condition (fig. S3A; $P < 10^{-27}$, Fisher's exact test). This finding mirrors a previous observation from analysis of the global genetic interaction network where hypomorphic alleles of proteasome genes show positive genetic interactions, which likely reflects reduced degradation of the products of TS alleles, providing a growth advantage (11). Similarly, ~6-fold more TS alleles showed positive differential fitness, relative to those with a negative differential fitness, when grown in sorbitol, which may reflect a general effect of increased intracellular osmolarity (fig. S3B; $P < 10^{-13}$, Fisher's exact test)(27). In contrast, TS alleles of essential genes were depleted for positive differential fitness effects in certain conditions, including growth in the presence of the *HSP90* inhibitor, Geldanamycin (fig. S3A; $P < 10^{-4}$, Fisher's exact test). This suggests that the fitness of different TS mutants is dependent on *HSP90* activity, which is consistent with the known role of *HSP90* as a phenotypic capacitor (11, 28–30).

Finally, we compiled a list of ~350 dynamic, "condition-responsive" genes, corresponding to the top ~5% of all tested genes based on the number of conditions in which they showed either a significant positive differential fitness score in 2 or more conditions or a significant negative differential fitness score in 4 or more conditions (Data File 1)(20). Consistent with our findings, condition-responsive genes identified in our assay were also often sensitive to multiple chemicals when assayed as homozygous gene deletion mutants (fig. S3C; 2.7-fold, $P < 10^{-12}$, Fisher's exact test)(31). Moreover, condition-responsive genes were more likely to be essential or to have a significant growth phenotype as a deletion mutant in the reference condition, were often highly connected on the global yeast genetic interaction network, and often encode highly conserved, multifunctional proteins (fig. S3D).

Mapping genetic interactions across different environments

Our systematic assessment of GxE interactions involving single mutants provides a foundation for comprehensive analysis of how genetic interactions are modulated by environment (GxGxE interactions). To do this, we took advantage of a diagnostic array used previously to survey complex, trigenic interaction networks (Data File 1)(6, 20). This array consists of ~1,200 strains, comprising ~1,000 nonessential gene deletion mutants and ~200 TS alleles of essential genes, spanning ~20% of all yeast genes and representing the functional breadth of the yeast genome (Data File 1)(6, 20). We note that mutant strains included on the diagnostic array exhibited a range of fitness defects and are generally representative of the genome-wide distribution of differential single mutant fitness effects (Data File 1)(20). For condition-specific genetic interaction analysis, we selected 26 query genes, each of which shows a substantial number of genetic interactions in the global network (11) and a functionally coherent genetic interaction profile that localizes the query gene to a specific biological process cluster on the reference genetic interaction similarity network (Fig. 1B).

We crossed the 26 query strains to the diagnostic mutant array resulting in ~30,000 unique double mutant strains, which were each assessed for environmental modulation of genetic

interactions in all 14 conditions. To measure condition-dependent genetic interactions, every double mutant array generated from a single query gene was screened 3 times. One copy was grown in the standard SGA condition, while the two other copies were each grown in different conditional media (fig. S4). This configuration provided a matched reference control for every condition, which facilitated normalization of systematic experimental artifacts and improved accuracy of condition-specific genetic interaction measurements (32). The entire screening pipeline was repeated twice, providing two independent biological replicates for every query gene in every test condition, each one with 4 separate double mutant colonies (8 tests of each double mutant per condition), and 14 independent biological replicates of each query screen in the standard reference SGA condition (23).

Negative and positive genetic interactions were quantified as previously described (19). We identified an average of ~2,100 negative and ~1,400 positive genetic interactions on the basis of 14 biological replicate screens performed in the standard, reference condition, at an intermediate confidence threshold (fig. S5A, Data File 3)(20, 23). A similar number of gene pairs exhibited a genetic interaction in any single test condition, with an average of ~2,150 negative and ~1,500 positive genetic interactions identified per condition (fig. S5A). Our genetic interaction measurements were reproducible, and those interactions identified in the reference condition in this study overlapped substantially with interactions derived from our previous genome-wide study (fig. S5B)(11). Comparison of the overlap of genetic interaction profiles between a specific condition screen and its matched control to that seen with an unmatched control suggested that comparison to a matched reference provides the necessary sensitivity to detect rare condition-specific interactions (fig. S5C, Table S1-S2, Data File 3)(20), consistent with previous studies (32).

Quantifying and classifying differential interactions

To discover differential or GxGxE interactions in our scored data, we quantified the difference between genetic interaction scores derived from each conditional screen and its corresponding matched reference (fig. S4)(23). We scored a differential negative interaction when a genetic interaction score observed in a particular condition was less than the genetic interaction score measured in the corresponding reference control. Conversely, a genetic interaction that was stronger in a given condition compared to the matched reference control was scored as a differential positive interaction. Analysis of biological replicates confirmed the reproducibility of differential interaction scores and enabled scoring of dynamic, differential genetic interactions while controlling for the false discovery rate (fig. S5D, Table S1-S2)(23).

The Benomyl screen showed the largest number of differential, condition-specific fitness defects and genetic interactions, providing a rich context for developing a general scheme for defining various classes of differential interactions. We measured Benomyl differential interactions as described above, adopting an intermediate confidence threshold ($|\varepsilon| > 0.08$, $P < 0.05$, see Method Summary and (23) for details)(Fig. 2A, left panel). In total, we identified 1,367 differential interactions in Benomyl, which was ~3-fold less than the 3,845 genetic interactions identified in the matched reference condition (Fig. 2B). Thus, the majority of the genetic interactions observed in the reference condition were also

observed in the presence of Benomyl. To determine if the prevalence of Benomyl differential interactions derived from the diagnostic array was generalizable to the whole genome, we also screened the same set of 26 SGA query mutant strains against the complete collection of nonessential gene deletion mutants and essential gene TS alleles, in the absence or presence of Benomyl (fig. S6A-B, Data File 3)(20, 23). This analysis also revealed ~3-fold fewer differential interactions relative to genetic interactions indicating that trends observed with the diagnostic array accurately reflect an unbiased genome-scale analysis (fig. S6C).

In an effort to discover what new functional information might be associated with differential interactions, we divided them into four classes: reversed, modified, masked and novel (Data File 3)(20, 23). These classes of differential interactions can be depicted schematically for those with either negative (Fig. 2A, right panel) or positive (fig. S7A) scores. The reversed class was the rarest and included gene pairs that showed significant but opposite genetic interactions in a condition versus the matched reference, accounting for less than 1% of all Benomyl differential interactions (Fig. 2B). Often these differentials involved at least one relatively weak interaction, which means they are likely more prone to false positives and false negatives. Thus, the sign of a fitness-based genetic interaction does not frequently change in an altered environment. The remaining classes were roughly equivalent in size and accounted for the majority (> 99%) of all Benomyl differential interactions (Fig. 2B, Data File 3)(20). We identified 538 (538/1,367; ~39%) novel differential interactions, which were not observed as genetic interactions in the reference network. The remaining (829/1,367; ~61%) differential interactions were either modified or masked, meaning that they were scored as genetic interactions in a particular condition as well as in the reference control, but differed in relative strength, and thus were modulated by the environment. Genome-wide analysis revealed similar fractions of modified, masked and novel Benomyl differential interactions (fig. S6D).

Analysis of specific examples of modified differential interactions from the Benomyl screens revealed that modified differential interactions could arise in two ways (Fig. 2A, fig. S7A). First, a genetic interaction detected in the reference network may be exacerbated in a specific condition, resulting in a significant differential score. For example, a negative genetic interaction between *MYO2* and *DYN2* was stronger in Benomyl, reflecting the importance of these two motor proteins in nuclear positioning and spindle orientation, especially when microtubule function is compromised (Fig. 2B). In another example, a positive genetic interaction between the proteasome gene, *RPN12,* and *TCP1,* which encodes an essential subunit of the chaperonin-containing T-complex involved in tubulin folding (Fig. 2B), was enhanced in the presence of Benomyl. In this case, compromising proteasome function may impair the degradation of the *TCP1* TS allele product, which is particularly important in the presence of Benomyl.

Second, a negative differential score may arise when a positive genetic interaction in the reference network is weakened in a specific condition (Fig. 2A, fig. S7A). For example, a positive genetic interaction between *GIM3* and *RPN12,* which encode subunits of the Prefoldin chaperone complex and the 19S proteasome, respectively, was weaker in the presence of Benomyl, resulting in a negative differential score (Fig. 2B). Similarly, a positive differential score can result from a condition-specific change in magnitude of

a negative genetic interaction. For example, in the reference condition, *GIM3,* which is involved in tubulin folding, showed a relatively strong negative genetic interaction with *DAD1*, an essential kinetochore gene (Fig. 2B). In Benomyl, the *GIM3-DAD1* negative genetic interaction was significant but much weaker, resulting in a differential positive interaction (Fig. 2B), which may reflect that Benomyl perturbs the microtubule cytoskeleton in a manner that encompasses the cell physiology associated with the *GIM3-DAD1* interaction.

We also categorized a specific subset of modified differential interactions, which we call 'masked', where positive or negative genetic interactions were only identified in the reference condition (Fig. 2A, fig. S7A). For example, while a negative genetic interaction was scored in the reference condition for *GIM3* and *TUB3*, which encodes alpha-tubulin, no genetic interaction was observed in the presence of Benomyl, leading to a *GIM3-TUB3* differential positive interaction (Fig. 2B). Positive genetic interactions scored in the reference condition can also be masked. For example, a positive genetic interaction between the yeast actin gene, *ACT1,* and the microtubule motor encoding gene, *KAR3,* was no longer detectable in Benomyl, leading to an *ACT1-KAR3* differential negative interaction (Fig. 2B).

Although relatively rare, novel differential interactions are particularly interesting because they are revealed only in a specific condition but not in the reference condition, and thus should reflect functional links between genes that are driven by condition-dependent cellular physiology (Fig. 2A, fig. S7A). For example, we identified a novel negative differential interaction between *DSN1* and *KIP3* in Benomyl highlighting a functional link between the kinetochore and a microtubule motor protein involved in spindle assembly (Fig. 2B).

Multiple environments, differential interactions, and the reference genetic network

We applied our scoring and classification system for differential genetic interactions, described above, to all 14 conditions surveyed. On average, less than 3% of all gene pairs tested in any given condition showed a differential interaction as compared to ~13% of all gene pairs that exhibited a genetic interaction in the reference condition, consistent with the percent of overlapping gene pairs that show a genetic interaction in the context of a genome-wide study (fig. S7B-C, Data File 3)(11, 20). Comparison of negative interactions, in particular, revealed a striking difference where ~1% of tested gene pairs exhibited a significant differential negative interaction, relative to ~8% of all gene pairs that showed a negative genetic interaction in any single condition tested (Fig. 3A, S7C, Data File 3)(20). Importantly, two-thirds of all differential interactions were classified as modified or masked because they overlapped a genetic interaction in the reference condition (Fig. 3B). On average, modified and masked differential interactions from a single condition accounted for ~14% of all genetic interactions in the reference network (Fig. 3B). Depending on the condition, we estimate that between ~5–24% of genetic interactions detected in a reference genetic network can be modulated in a different environment.

Novel differential interactions provide a direct estimate of the additional functional information that different environments can contribute to a genetic network. On average, when compared to a matched reference control, ~7% of genetic interactions identified in a single condition were classified as novel differential interactions (Fig. 3B, Data File 3)(20). Thus, the vast majority (~93%) of the genetic interactions mapped in different environmental conditions were also on the reference network. Novel differential negative interactions were also significantly weaker in magnitude compared to genetic interactions measured in the reference condition (Fig. 3C). Detailed analysis of previously reported differential interaction networks (14, 15, 17) confirmed that differential interactions, in particular, novel differential interactions, were much less abundant than genetic interactions (fig. S7D).

It is critical to account for the false negative rate associated with high-throughput genetic interaction screens because failure to detect a true reference condition genetic interaction can be mistakenly classified as a novel differential interaction. We applied a Markov Chain Monte Carlo (MCMC)-modelling approach to generate a robust consensus set of negative and positive reference condition genetic interactions for each of the 26 SGA query genes based on the collection of 14 independent, biological replicate screens (23). The resultant consensus genetic interaction profiles were used as a gold-standard to estimate false discovery and false negative rates at defined confidence thresholds (Table S1-S2; Data File 4)(20). From analysis of reference condition replicate screens, we estimated false negative rates of 39% and 52% for negative and positive genetic interactions, respectively (Table S1)(23). In the case of Benomyl, we mapped 538 novel differential interactions when compared to a reference condition network derived from a single, matched control (Fig. 3D, fig. S7C). However, a more rigorous comparison of Benomyl genetic interactions versus the MCMC consensus reference genetic interaction profile identified 454 novel differential interactions or ~15% fewer interactions than comparison to a matched control screen (Fig. 3D). A third comparison using a saturated reference network, on the basis of a reference network derived from the union of all the control screens (fig. S7E), which is less prone to false negative interactions, identified 319 novel differential interactions, or ~40% fewer interactions compared to those identified using a single matched reference control (Fig. 3D)(23). Indeed, the number of novel differential interactions could decrease by as much as ~60% depending on the condition and whether the reference was based on a single matched control, a consensus network control (23), or the union of reference control screens (Fig. 3D; Data File 4)(20). Our analysis highlights the importance of a robust reference network, replicate screens and rigorous estimates of false negative rates for comparative study of genetic interactions in an alternative environmental condition.

Properties of differential interactions

Comparing all 14 conditions to their matched controls identified a combined total of ~10,000 differential interactions, the majority (61%) of which were unique to a single growth condition, with differential negative interactions being less prevalent and relatively weaker than differential positive interactions (Fig. 3B, fig. S7F). Genes that were highly connected hubs on the global genetic network were also more likely to be hubs on a differential network, since the average number of differential interactions for an individual array gene, across all 14 conditions, was significantly correlated to the interaction degree

in the global genetic network (Pearson correlation, $r = \sim 0.7$, $P < 10^{-16}$, fig. S8A, B). The number of novel differential interactions associated with each query mutant examined in this study was also correlated to interaction degree in the global genetic network (Pearson correlation, $r = \sim 0.5$, $P < 0.006$, fig. S8C), suggesting that the frequency of novel differential interactions observed using a diagnostic set of genes should reflect the genome-wide prevalence of novel differential interactions. Consistent with these observation, gene features associated with hubs on the reference network were shared with differential network hubs (fig. S8D)(11). Notably, high novel differential interaction degree was associated with genes whose loss-of-function resulted in a single mutant fitness defect in the reference condition (fig. S8E), and genes with condition-dependent fitness defects had proportionally more novel differential interactions than genes lacking condition-dependent fitness defects (fig. S8F). Like genetic interaction hubs, genes with many novel differential interactions were associated with multiple Gene Ontology (GO) annotations, and lower dN/dS suggesting that they are more functionally pleiotropic and tend to be under stronger evolutionary constraints (fig. S8D-E). Conversely, transcript levels of high differential interaction degree genes did not vary substantially across different environments or genetic backgrounds, suggesting that environmentally responsive gene expression patterns are not generally predictive of differential interactions (fig. S8D).

Negative genetic interactions measured in any condition tended to connect functionally related gene pairs and overlapped with other types of molecular interaction networks (Fig. 4A-B). Differential negative interactions also identified functionally related gene pairs, but to a lesser extent (Fig. 4A-B). Closer examination revealed that most of the functional signal associated with differential negative interactions was captured by the modified class, whereas those belonging to the novel or masked categories did not overlap substantially with other molecular interaction datasets (Fig. 4B). Thus, negative genetic interactions that occurred in a condition-specific manner (i.e. novel differential negative interaction; Fig. 2A), and positive genetic interactions that are masked in a particular condition (i.e. masked differential negative interaction; Fig. 2A) often involve gene pairs with unrelated functional annotations.

Consistent with previous observations (11), positive genetic interactions identified in either the reference or alternative conditions were less functionally informative than negative genetic interactions (Fig. 4A, C). However, the complete set of differential positive interactions appeared to connect functionally related genes more often than positive genetic interactions measured in either the reference or individual test conditions (Fig. 4C). Modified and masked differential positive interactions were the most predictive of functionally related gene pairs, often connecting members of the same protein complex and overlapping significantly with protein-protein interactions (Fig. 4B). Further analysis revealed that the functional signal associated with the masked and modified classes was largely attributable to gene pairs that displayed negative genetic interactions in the reference condition but were either weaker (modified) or no longer detectable (masked) in a particular condition (Fig. 4D). This may reflect a particular environmental perturbation that mimics the cellular physiology associated with a double mutant strain grown in the reference condition, obscuring a phenotype associated with a genetic interaction. Thus, while modified and masked differential positive interactions tend to connect functionally related gene pairs, this

same information is captured by negative genetic interactions identified in the reference condition. We note that genome-wide analysis revealed similar functional trends associated with Benomyl differential negative and positive interactions (fig. S6E-F).

To further explore the functional information associated with condition-specific interactions, we grouped together array genes that belong to the same biological process cluster represented on the global genetic profile similarity network (Fig. 1A) and measured how often each query gene showed either genetic or novel differential interactions with each functional group (Fig. 5, Data File 5)(11, 20, 23). Query and array genes within the same bioprocess cluster were often connected by negative genetic interactions in the reference condition (~3.6-fold enrichment within bioprocess, Fig. 5A, on-diagonal). For example, in the reference condition, the *VTI1* query gene, which encodes an essential SNAP receptor (v-SNARE) involved in multiple protein sorting pathways (33–35) and located in the vesicle traffic bioprocess cluster, showed strong enrichment for negative genetic interactions with functionally-related array genes located in the same vesicle traffic bioprocess cluster (Fig. 5B).

In contrast, novel differential negative interactions did not connect query and array genes annotated to the same biological process (Fig. 5C). While *VTI1* showed the most novel differential interactions of any query gene tested (Data File 3)(20), most of these interactions did not involve other vesicle traffic-related genes. Instead, we observed modest but significant enrichment for novel differential negative interactions between the *VTI1* query gene and array genes with roles in cell polarity and nuclear transport (Fig. 5D). Indeed, the vast majority (1489/1553, ~96%) of all novel differential negative interactions identified using a matched reference control connected pairs of genes located in different bioprocess clusters on the global similarity network. These results further indicated that condition-specific genetic interactions do not identify gene pairs with a close functional relationship in the same general bioprocess but rather have the potential to uncover weaker functional associations between distinct biological processes.

Differential interactions capture distant but coherent functional relationships

We next explored the functional distribution of novel differential interactions across each of the 14 different conditions. In particular, we tested if array genes annotated to the same function showed more novel differential interactions in a particular condition (Fig. 6). Array genes annotated to specific biological processes were enriched for novel differential negative interactions in response to a specific condition that perturbs the same bioprocess (~2.3-fold enrichment within bioprocess; Fig. 6A, on-diagonal). For example, consistent with previous observations (14, 15), we found that array genes in the DNA replication and repair bioprocess cluster were enriched for novel differential negative interactions in the presence of MMS (3.9-fold, Fig. 6B). But as shown above (Fig. 5), these novel differential interactions did not involve related query genes with roles in DNA replication and repair. The enrichment observed among DNA replication and repair array genes was predominantly driven by MMS-specific, novel differential negative interactions with the

MYO2 query gene, a type V myosin motor involved in actin-based vesicle transport and spindle orientation, and with the *VTI1* and *TRS20* query genes involved in vesicle transport, highlighting a functional link between DNA replication and vesicle trafficking (Fig. 6B)(33–35). In another example, vesicle traffic genes were enriched for novel differential negative interaction in response to Monensin (2.5-fold, Fig. 6A). In this case, Monensin-specific negative interactions connected vesicle traffic array genes to the *RSP5* query gene, which encodes a ubiquitin ligase involved in multi-vesicular body sorting, the heat shock response, endocytosis, and ribosome assembly (36), as well as the *LSM6* query gene, which has a general role in RNA processing (Fig. 6B)(37, 38). Novel differential positive interactions were also not enriched among functionally related genes, and they were less informative of gene function than novel differential negative interactions (fig. S9A, Data File 5)(20).

A similar trend was observed in genome-scale Benomyl screens, where novel differential negative interactions specifically connected array genes with mitosis-related roles to functionally diverse query genes, such as *NUP188*, which encodes a nuclear pore component (39), and *GPI15*, involved in glycosylphosphatidylinositol (GPI) anchor biosynthesis (fig. S9B, Data File 5)(20, 40, 41). Thus, environment may sensitize genes with roles in a specific bioprocess to negative genetic interactions with functionally diverse query genes.

In summary, the majority of differential interactions overlap a genetic interaction identified in the reference condition, which often connect functionally related genes within the same biological process. The environmental rewiring of genetic networks is driven by rare condition-specific, and relatively weak novel differential interactions, which identify new connections between genes with diverse functions in different biological processes (Fig. 7).

Discussion

We surveyed a set of functionally diverse yeast genes and different environments, quantifying how the growth phenotypes associated with different single gene mutations were modulated by the environment (GxE), and how the growth phenotypes associated with different genetic interactions (GxG) respond dynamically to a particular condition to generate differential interactions (GxGxE). Our general findings reveal how environmental conditions modulate the yeast global genetic interaction network, allowing us to assess the plasticity of genetic networks, and the extent to which mapping genetic interactions in different environments can expand a reference network and generate new functional information.

In general, genetic interactions, especially negative genetic interactions, are rich in functional information because they tend to connect genes that function within the same biological process (GxG, Fig. 7)(11). Analogously, if an environmental perturbation affects a particular biological process, then genes with roles in the perturbed bioprocess tend to show differential sensitivity in the corresponding condition (GxE, Fig. 7). Most genetic interactions are not modulated by the environment and remain detectable in both a given test condition and the reference control condition. However, subsets of genetic interactions can be modified by a particular condition, leading to a differential interaction (GxGxE, Fig. 7).

Differential interactions are relatively rare because, on average, we observed ~3-fold fewer differential interactions compared to genetic interactions detected in the reference condition.

Most differential interactions belonged to the modified or masked classes, which overlapped with a negative or positive genetic interaction in the reference genetic network. The majority (~70%) overlapped specifically with negative genetic interactions and thus were functionally informative, connecting genes belonging to the same general biological process (GxGxE – e.g. modified, Fig. 7). However, because they recapitulate connections that are captured in the global genetic network mapped in the reference condition, modified and masked differential interactions do not contribute new functional information. On the other hand, novel differential interactions correspond to condition-specific genetic interactions between genes that do not interact in the reference condition. The rare sub-class of novel differential negative interactions does not typically include functionally related gene pairs. Instead, these interactions tend to connect groups of genes that are sensitive to a particular environmental perturbation to functionally distant genes (GxGxE – novel, Fig. 7). Thus, novel differential interactions highlight new connections between distinct cellular functions and, as a result, have the potential to expand upon the global genetic network.

Although detecting novel differential interactions promises to add new information to genetic networks, an accurate definition of novel differential interactions is challenging as it depends on the quality and comprehensiveness of the reference genetic network. For example, multiple independent replicate screens reduce the number of false negative interactions observed in the reference condition but consequently, also decrease the number of differential interactions classified as novel upon environmental perturbation (Fig. 3D). Indeed, the relative fraction of novel differential interactions contributed to the reference network by a single environmental condition can vary widely when using a single, matched control (~7%) or the union of all available replicate controls (~1%)(Data File 4)(20). Using a high confidence consensus reference network (Data File 4)(20), we estimate that screening one additional environmental condition contributes less than ~4% (191/5174) novel interactions relative to the reference network, suggesting that most genetic interactions are captured in a single condition. Hence, while differential interaction analysis in multiple diverse conditions reveals the subset of genetic interactions that are modulated upon environmental perturbations (i.e. modified or masked interactions), they can only marginally expand the size of the network (i.e. novel interactions) highlighting that the global genetic interaction network is generally robust to environmental perturbations.

While our study involved the use of a diagnostic array of yeast genes, selected environmental conditions and functionally diverse query genes, several observations suggest that our results capture the general resilience of the global yeast genetic interaction network to environmental perturbation. First, our genome-scale single mutant fitness analyses suggested that the selected set of conditions and small molecules elicited widespread but distinct cell physiological effects. Second, a genome-wide comparison of genetic interactions measured in the absence and presence of Benomyl yielded a similar fraction of differential interactions seen using a diagnostic mini-array of genes. Finally, analysis of several independent interaction datasets, derived from SGA-based approaches using various subsets of yeast genes and a number of different conditions, including various DNA

damaging agents and stress-response conditions, confirmed that differential interactions are substantially less prevalent than the genetic interactions observed in the reference condition (fig. S7D) (14, 15, 17).

Consistent with our results, previous surveys of subsets of genes involved in a specific cellular function perturbed by a particular condition revealed an enrichment for differential interactions that often occurred between functionally distant gene pairs (14, 15, 17). We note that, although included in previous studies, a subset of differential interactions, based on statistically insignificant genetic interaction scores, was omitted from our analysis (23). However, these particular differential interactions were not enriched among functionally related genes and did not appreciably increase the total number of differential interactions relative to the size of the reference genetic interaction network examined here or reported in other studies (fig. S7D, S10). Thus, in general, genetic interactions between the vast majority of genes and their corresponding functional modules (e.g. complexes and pathways) are not dynamic or rewired in response to environmental stimuli. Moreover, we found that the ~20% of yeast genes with relatively sparse genetic interaction profiles (11) are statistically depleted for condition-specific fitness defects (~3-fold depletion, $P < 10^{-99}$, Fisher's exact test, one-tailed). The relationship between fitness and interaction degree (fig. S8) along with the strong correlation observed between interaction degree for a given gene in the global genetic and differential networks (fig. S8), further suggests that condition-specific genetic interactions will not appreciably increase the number of interactions associated with low degree genes in the global reference genetic network.

Differential interactions reflect the phenotypic consequences of combining three independent perturbations, two genetic and one environmental perturbation, and thus conceptually resemble trigenic interactions, which involve three independent genetic perturbations, especially if a condition involves a drug with a highly specific cellular target. As a result, differential and trigenic interaction networks share several properties in common: [1] As observed for differential interactions, the average trigenic interaction degree for a given gene was correlated to its connectivity in the global genetic network (6); [2] Like novel differential interactions, trigenic interactions occur at similar reduced frequencies relative to digenic interactions in a reference condition (fig. S7D); [3] Like modified and masked differentials, a substantial proportion of trigenic interactions overlapped with and exacerbated digenic interactions previously observed in the global digenic network (6); [4] As observed for novel differential interactions, novel trigenic interactions are also relatively rare and weaker, but highly coherent in that they often involve array genes from the same biological process; however, and they are also substantially more functionally diverse than digenic interactions (6).

GxE and GxGxE interactions involving the natural variation of different yeast strains can also be interpreted in the context of the global genetic interaction network and the properties of novel differential interactions. Using segregating populations of natural yeast isolates, recent surveys of GxG and GxGxE interactions between a deletion mutant and natural genetic variants showed that GxG interactions tend to connect genes within the same cellular function (42), whereas GxGxE interactions tend to be specific to a particular condition (43), and they often connected distantly related genes (44).

Quantitative trait loci (QTL) studies, focused on the fitness variation of different segregants derived from yeast crosses in different environments, showed that the majority of the phenotypic variation can be explained by single-locus effects (GxE), whereas epistatic genetic interactions, analogous to GxGxE interactions, are relatively rare (4, 45), and tend to impact only individuals with extreme phenotypes (5). Based on our analyses, most GxGxE interactions involve genes with single mutant differential effects (GxE) (fig. S8E), which should be analogous to single-locus effects identified in QTL analyses and contribute to both the additive and epistatic variance. In other words, the low epistatic variance often seen in QTL analyses may be partly explained by the partial contribution of interacting loci to the additive variance component (46). As a result, the remaining epistatic effect may only be visible in individuals with the most extreme phenotypes (5). Given that most GxGxE interactions overlap a genetic interaction in the global genetic interaction network, applying principles and gene modules inferred from a global network should allow for the detection of coherent epistatic interactions with relatively small effects that cannot be recovered using QTL analyses (47, 48).

We conclude that the yeast genetic interaction map derived from a single reference condition is highly robust to environmental influences because most connections on the global genetic interaction network remain unchanged or unmodified in a new environment. Although each new condition has the potential to map a relatively small number of novel differential interactions, the global digenic network mapped in a single condition is informative of differential interactions (fig. S8A-B) and should serve as an accurate and representative reference network. Nonetheless, differential interactions can reveal new functional connections between distantly related genes and bioprocesses. Given the significant association between the differential single mutant fitness defect and the frequency of differential interactions for a given gene, a logical and efficient strategy may involve mapping differential interactions for specific genes required for normal growth in a environment of interest (i.e. stress condition, drug treatment, microbial exposure etc.).

While environment has a modest impact, cell type-specific gene regulation has the potential to substantially complicate genetic network analyses in more complex systems. However, genome-wide studies suggest that only ~8,500 genes (~45–49%) are expressed in any given cancer cell line and that a “core set” of ~7,700 genes are expressed in the majority of all cancer cell lines examined to date (49). Thus, a systematic survey of genetic interactions based on a single cell line grown in one environment should be sufficient to map a global reference genetic network that encompasses this core set of expressed genes and provide a basic scaffold for the genetic wiring of a human cell. As observed in yeast, a global genetic interaction network for a model human cell line should reveal a hierarchy of functional connections among genes (1, 11), and expansion of this network to specific cell types would enable the deciphering of mechanisms underlying cancer cell-specific genetic vulnerabilities (50, 51). Ultimately, reference genetic networks mapped in human cells should facilitate interpretation of allelic combinations of genes underlying inherited traits (3, 47, 48).

Methods Summary

Non-essential deletion and essential TS mutant arrays

The complete nonessential gene deletion and essential gene TS allele arrays were used for all single mutant fitness and single mutant differential fitness (GxE) analyses and are described elsewhere (11).

Diagnostic mutant array

Unless otherwise noted, genetic and differential interactions were based on analysis of query mutant strains crossed to a previously described, functionally representative diagnostic array comprising 1,209 mutant strains (6). These included 1,012 nonessential deletion mutant array (DMA) strains (labeled_dma#), and 197 essential TS allele array (TSA) mutant strains (labeled_tsa#). A complete list of diagnostic mutant strains used in this study is provided (Data File 1)(20).

Query mutant strains

The set of 26 query mutant strains selected for this study were previously shown to have rich genetic interaction profiles that can recapitulate major bioprocess-enriched clusters on the genetic interaction profile similarity network and thus are representative of the global yeast genetic network (11, 52). SGA query strain construction was conducted as described previously (53). A list of query mutant strains used in this study is provided (Data File 1)(20).

Conditions

A list of 14 conditions and concentrations used in this study are provide in Data File 1(20).

SGA screening procedure

SGA experiments and selection steps were conducted as previously described (11, 53) with the following modifications. To measure condition-dependent genetic interactions, every double mutant array generated from a single query SGA screen was copied 3 times. One copy was grown in the standard SGA reference condition, while the two other copies were each grown in different conditional media (fig. S4). This configuration provided a matched, reference control for every condition, which facilitated normalization of systematic experimental artifacts and improved accuracy of condition-specific genetic interactions measurements, as described below. Because every double mutant array could be replicated a maximum of 3 times, each of the 26 query mutant strains was independently screened against the diagnostic array seven times allowing us to measure digenic interactions in 14 different test conditions (i.e. 2 test conditions + 1 reference condition/screen x 7 screens/query strain)(fig. S4). The entire screening pipeline was repeated twice resulting in independent biological replicates for each query screen in every test condition along with 14 biological replicates of each query screen in the standard, reference SGA condition. We also repeated screens for a subset of 4 query mutant strains (Data File 3)(20), where double mutant arrays were copied two times and each copy was grown in the standard

SGA reference condition to measure the reproducibility of genetic interactions derived from matched, reference control screens (fig. S5C).

Single mutant fitness scores

To derive accurate estimates of single mutant fitness, we applied our colony size scoring method (54) to a set of control SGA screens, where a query strain carrying a *natMX* marker inserted at a neutral genomic locus was crossed to the *kanMX*-marked DMA (_dma#) and TSA (_tsa#) strain collections. Colony size measurements of SGA deletion and TS array mutant strains were based on an average of 3 replicate control screens conducted per each of 14 test conditions as well as the reference condition at 26°C. Colony size measurements were used to estimate single mutant fitness in each condition as described previously (54) with the exception that bootstrapped means, instead of medians, across replicates were used in variance estimation and final fitness values. Due to technical reasons, single mutant fitness for a small subset of mutant strains (0.15% – 1.0% of all strains) are not reported.

Single mutant Differential fitness scores

To obtain condition specific fitness estimates, we computed the difference in colony size measured in a particular test condition versus the matched reference condition for each mutant. Single mutant fitness and differential fitness interaction data corresponding to all mutants represented in the DMA and TSA collections is provided as Supplementary data (Data File 1)(20). Due to technical reasons, single mutant fitness for a small subset of mutant strains (0.15% – 1.0% of all strains) are not reported.

Genetic interaction score

To derive quantitative genetic interactions, we modeled colony size as a multiplicative combination of double mutant fitness, time, and experimental factors as previously described (11, 19). Briefly, for a double mutant carrying mutations of genes i and j, colony size C_{ij} can be expressed as $C_{ij} = f_{ij} \cdot t \cdot s_{ij} \cdot e$, where f_{ij} is the double mutant fitness, t is the incubation time, s_{ij} is the combination of all systematic factors, and e is log-normally distributed random noise. The double mutant fitness f_{ij} can be further expressed as $f_{ij} = f_i f_j + \varepsilon_{ij}$, where f_i and f_j represent the fitness of the two single mutants and ε_{ij} is a quantitative measure of the genetic interaction (genetic interaction score) between them.

Genetic interaction data corresponding to all tested gene pairs identified in the reference and 14 different conditions is provided as Supplementary data (Data File 3)(20). The data should be filtered prior to use. We suggest two different thresholds [intermediate ($P < 0.05$ and $|\varepsilon| > 0.08$), and stringent confidence ($P < 0.05$ and $|\varepsilon| < 0.12$) that strike different balances between false negatives and false positives as described in our previous studies (11, 12). While the majority of query mutant strains were screened in all test conditions, a smaller subset of query mutants could not be screened in all 14 conditions due to technical and data quality control reasons. In total, 22/26 of query mutants were screened in at least 12 test conditions while 5 query mutants were screened for genetic interactions in less than 12 test conditions.

Differential interaction Score

To score differential genetic interactions, genetic interaction scores derived from each condition were matched with a paired reference condition. Additionally, we used genetic interaction scores from the previously published reference genetic interaction network (11), termed “global” in the section below to normalize screen data before differential interaction scoring. The first step in scoring differential interactions was to apply a correction to each query, condition, and replicate screen that normalized the genetic interaction scores such that the corrected standard deviation for overlapping gene pairs matched the published genetic interaction network. We performed this per condition, per query, per replicate correction on reference (untreated) and condition (treated) scores as follows:

$$\text{correction}_{c,q,r} = \frac{\sigma\left(\varepsilon_{\text{untreated},c,q,r}\right)}{\sigma\left(\varepsilon_{\text{global},c,q}\right)}$$

$$\hat{\varepsilon}_{\text{untreated},c,q,r} = \text{correction}_{c,q,r} \times \varepsilon_{\text{untreated},c,q,r}$$

$$\hat{\varepsilon}_{\text{treated},c,q,r} = \text{correction}_{c,q,r} \times \varepsilon_{\text{treated},c,q,r}$$

where c is the condition, q is the query, r is the replicate, ε is the uncorrected epsilon score, σ is the calculated standard deviation of the reference condition (untreated) epsilon scores for that query, condition (treated) and replicate, or the global epsilon scores for that condition and query from our previous work (11) and $\hat{\varepsilon}$ is the corrected epsilon score. This conforms the variance of interaction measurements in each condition to a fixed reference and facilitates comparisons of interaction density across different conditions. Note that each condition (treated) network has a paired reference (untreated) network, which is used to compute the correction factor above.

Three replicate scores were collected for every differential genetic interaction measurement. Some screens resulted in missing data for certain pairs due to data quality issues or strong fitness defects in the screened conditions. To mitigate the effect of missing data, we only considered interactions for which we had at least two replicate measurements. For interactions that had three replicates, we selected the two replicates with the highest correlation of corrected differential interaction scores for each query-condition pair.

We found that screening genetic interactions in compound stress conditions increased the variance in genetic interaction estimates. In order to mitigate this effect, we applied a variance stabilization correction to further correct conditional epsilon scores.

$$\text{variance stabilization}_c = \frac{\sigma\left(\left|\hat{\varepsilon}_{\text{untreated},c,r=1} - \hat{\varepsilon}_{\text{untreated},c,r=2}\right|\right)}{\sigma\left(\left|\hat{\varepsilon}_{\text{treated},c,r=1} - \hat{\varepsilon}_{\text{treated},c,r=2}\right|\right)}$$

$$\hat{\hat{\varepsilon}}_{\text{treated},\,c,\,q,\,r} = \text{variance stabilization}_c \times \hat{\varepsilon}_{\text{treated},\,c,\,q,\,r}$$

where c is the condition, q is the query, r is the replicate, $\hat{\varepsilon}$ is the corrected epsilon score, σ is the calculated standard deviation and $\hat{\hat{\varepsilon}}$ is the variance-stabilized, corrected treated epsilon score. After applying these normalizations, the differential score is calculated for each of the paired replicates separately, as follows:

$$\text{differential score}_r \times \hat{\hat{\varepsilon}}_{\text{treated},\,r} - \hat{\varepsilon}_{\text{untreated},\,r}$$

A final differential score, final untreated score, and final treated score are calculated from the mean of the two replicate differential scores, corrected untreated epsilon scores, and variance-stabilized, corrected treated epsilon score, respectively. Throughout these calculations, the standard deviations of the original measurements are propagated to derive an estimate of error on the final differential score. The resulting standard deviation is used to derive a *P* value for each differential interaction score, which was calculated as the two-sided probability of observing a more extreme score than the one measured given a background normal distribution centered on zero with a standard deviation equal to the one observed.

Differential interaction data corresponding to all tested gene pairs are provided as Supplementary data (Data File 3)(20). For analysis of individual interactions, we recommend that the data first be filtered prior to further analysis by applying one of our recommended thresholds (e.g. an intermediate threshold, $P < 0.05$ and $|\varepsilon| < 0.08$).

Classifying differential interactions

Differential interactions were categorized as either novel, modified or masked by comparing the genetic interaction scores for a given double mutant measured in a particular condition and the matched reference control (Fig. 2). Importantly, two additional categories of differential interactions were excluded from our analysis. First, gene pairs that did not show a significant genetic interaction ($P < 0.05$ and $|\varepsilon| < 0.08$) in either a given test condition, or the matched reference condition were excluded from further analysis as we could not be confident of a significant interaction in either the reference or the test conditions, individually, even though the differential score was significant. Second, double mutants that exhibited a significant and extreme negative genetic interaction ($P < 0.05$ and $|\varepsilon| < -0.3$) in both a condition and the matched reference control were considered synthetic lethal in both the reference and test conditions and also excluded from further analyses of differential interactions.

Evaluating functional relations captured by differential interactions

We explored the functional information associated with different types of genetic interactions based on Spatial Analysis of Functional Enrichment (SAFE) neighborhood enrichment analysis (11, 55). Query and mini-array genes were assigned to one of the 17 bioprocesses or neighborhoods on the global genetic interaction profile similarity map based on SAFE analysis (11, 55). For each query in each condition, we counted the number

of interacting array genes that occurred in each of the 17 SAFE neighborhoods. For query-centric analyses (Fig. 5), we summed up interactions associated with a specific query gene across all 14 conditions and calculated the fold enrichment for each neighborhood with a one-sided Fisher's exact test, by comparing the number of interacting array genes assigned to a given neighborhood vs. the total number of interactions with that particular query, using the fraction of array genes assigned to the same neighborhood across the mini-array as background. For condition-centric analyses (Fig. 6), we performed the same test by combining all queries within each tested condition. This analysis was performed for negative and positive genetic interactions (Fig. 5–6, fig. S9B), novel negative differential interactions (Fig. 5–6, fig. S9A) using the mini-array screens, and novel negative differential interactions using the genome-wide screen on Benomyl condition (fig. S9A).

A more detailed description of the experimental and computational analyses are provided as supplementary materials.

All Data Files associated with this study are available for download from: DRYAD (doi:10.5061/dryad.3r2280gfd) or https://boonelab.ccbr.utoronto.ca/condition_sga/

Supplementary Material

Refer to Web version on PubMed Central for supplementary material.

Funding:

This work was primarily supported by the National Institutes of Health (R01HG005853)(B.A., C.B., C.L.M.), Canadian Institutes of Health Research (FDN-143264 and FDN-143265)(C.B., B.A.), National Institutes of Health (R01HG005084)(C.L.M), the National Science Foundation (DBI\0953881)(C.L.M.) and a Ramon y Cajal fellowship (RYC-2017–22959)(C.P.). Computing resources and data storage services were partially provided by the Minnesota Supercomputing Institute and the UMN Office of Information Technology, respectively. C.B is a fellow of the Canadian Institute for Advanced Research (CIFAR).

References

1. Costanzo M et al. , Global Genetic Networks and the Genotype-to-Phenotype Relationship. Cell 177, 85 (2019). [PubMed: 30901552]
2. Phillips PC, Otto SP, Whitlock MC, in Epistasis and the evolutionary process, Wolf JB, Brodie EDI, Wade MJ, Eds. (Oxford University Press, 2000).
3. Zuk O, Hechter E, Sunyaev SR, Lander ES, The mystery of missing heritability: Genetic interactions create phantom heritability. Proc Natl Acad Sci U S A 109, 1193 (2012). [PubMed: 22223662]
4. Bloom JS, Ehrenreich IM, Loo WT, Lite TL, Kruglyak L, Finding the sources of missing heritability in a yeast cross. Nature 494, 234 (2013). [PubMed: 23376951]
5. Forsberg SK, Bloom JS, Sadhu MJ, Kruglyak L, Carlborg O, Accounting for genetic interactions improves modeling of individual quantitative trait phenotypes in yeast. Nat Genet 49, 497 (2017). [PubMed: 28250458]
6. Kuzmin E et al. , Systematic analysis of complex genetic interactions. Science 360, (2018).
7. Tong AH et al. , Systematic genetic analysis with ordered arrays of yeast deletion mutants. Science 294, 2364 (2001). [PubMed: 11743205]
8. Tong AH et al. , Global mapping of the yeast genetic interaction network. Science 303, 808 (2004). [PubMed: 14764870]

9. Mani R, St Onge RP, Hartman J. L. t., Giaever G, Roth FP, Defining genetic interaction. Proc Natl Acad Sci U S A 105, 3461 (2008). [PubMed: 18305163]
10. van Leeuwen J et al. , Exploring genetic suppression interactions on a global scale. Science 354, (2016).
11. Costanzo M et al. , A global genetic interaction network maps a wiring diagram of cellular function. Science 353, (2016).
12. Costanzo M et al. , The genetic landscape of a cell. Science 327, 425 (2010). [PubMed: 20093466]
13. St Onge RP et al. , Systematic pathway analysis using high-resolution fitness profiling of combinatorial gene deletions. Nat Genet 39, 199 (2007). [PubMed: 17206143]
14. Bandyopadhyay S et al. , Rewiring of genetic networks in response to DNA damage. Science 330, 1385 (2010). [PubMed: 21127252]
15. Guenole A et al. , Dissection of DNA damage responses using multiconditional genetic interaction maps. Molecular cell 49, 346 (2013). [PubMed: 23273983]
16. Kramer MH et al. , Active Interaction Mapping Reveals the Hierarchical Organization of Autophagy. Mol Cell 65, 761 (2017). [PubMed: 28132844]
17. Martin H et al. , Differential genetic interactions of yeast stress response MAPK pathways. Mol Syst Biol 11, 800 (2015). [PubMed: 25888283]
18. Jaffe M et al. , Improved discovery of genetic interactions using CRISPRiSeq across multiple environments. Genome Res 29, 668 (2019). [PubMed: 30782640]
19. Baryshnikova A et al. , Quantitative analysis of fitness and genetic interactions in yeast on a genome scale. Nat Methods 7, 1017 (2010). [PubMed: 21076421]
20. All Data Files are available from the DRYAD Digital Respository (doi:10.5061/dryad.3r2280gfd) as well as https://boonelab.ccbr.utoronto.ca/condition_sga/.
21. Winzeler EA et al. , Functional characterization of the S. cerevisiae genome by gene deletion and parallel analysis. Science 285, 901 (1999). [PubMed: 10436161]
22. Li Z et al. , Systematic exploration of essential yeast gene function with temperature-sensitive mutants. Nature biotechnology 29, 361 (2011).
23. Materials and Methods are available as supporting online material
24. Gasch AP et al. , Genomic expression programs in the response of yeast cells to environmental changes. Mol Biol Cell 11, 4241 (2000). [PubMed: 11102521]
25. Clark TA, Sugnet CW, Ares M Jr., Genomewide analysis of mRNA processing in yeast using splicing-specific microarrays. Science 296, 907 (2002). [PubMed: 11988574]
26. Tartakoff AM, Perturbation of vesicular traffic with the carboxylic ionophore monensin. Cell 32, 1026 (1983). [PubMed: 6340834]
27. Back JF, Oakenfull D, Smith MB, Increased thermal stability of proteins in the presence of sugars and polyols. Biochemistry 18, 5191 (1979). [PubMed: 497177]
28. Cowen LE, Lindquist S, Hsp90 potentiates the rapid evolution of new traits: drug resistance in diverse fungi. Science 309, 2185 (2005). [PubMed: 16195452]
29. Rizzolo K et al. , Features of the Chaperone Cellular Network Revealed through Systematic Interaction Mapping. Cell Rep 20, 2735 (2017). [PubMed: 28903051]
30. Queitsch C, Sangster TA, Lindquist S, Hsp90 as a capacitor of phenotypic variation. Nature 417, 618 (2002). [PubMed: 12050657]
31. Lee AY et al. , Mapping the cellular response to small molecules using chemogenomic fitness signatures. Science 344, 208 (2014). [PubMed: 24723613]
32. Bean GJ, Ideker T, Differential analysis of high-throughput quantitative genetic interaction data. Genome biology 13, R123 (2012). [PubMed: 23268787]
33. Dilcher M, Kohler B, von Mollard GF, Genetic interactions with the yeast Q-SNARE VTI1 reveal novel functions for the R-SNARE YKT6. J Biol Chem 276, 34537 (2001). [PubMed: 11445562]
34. Kim JJ, Lipatova Z, Segev N, TRAPP Complexes in Secretion and Autophagy. Front Cell Dev Biol 4, 20 (2016). [PubMed: 27066478]
35. Pruyne D, Legesse-Miller A, Gao L, Dong Y, Bretscher A, Mechanisms of polarized growth and organelle segregation in yeast. Annu Rev Cell Dev Biol 20, 559 (2004). [PubMed: 15473852]

36. Rotin D, Kumar S, Physiological functions of the HECT family of ubiquitin ligases. Nat Rev Mol Cell Biol 10, 398 (2009). [PubMed: 19436320]
37. Kaliszewski P, Zoladek T, The role of Rsp5 ubiquitin ligase in regulation of diverse processes in yeast cells. Acta Biochim Pol 55, 649 (2008). [PubMed: 19039336]
38. Beggs JD, Lsm proteins and RNA processing. Biochem Soc Trans 33, 433 (2005). [PubMed: 15916535]
39. Aitchison JD, Rout MP, The yeast nuclear pore complex and transport through it. Genetics 190, 855 (2012). [PubMed: 22419078]
40. Orlean P, Architecture and biosynthesis of the Saccharomyces cerevisiae cell wall. Genetics 192, 775 (2012). [PubMed: 23135325]
41. Barlowe CK, Miller EA, Secretory protein biogenesis and traffic in the early secretory pathway. Genetics 193, 383 (2013). [PubMed: 23396477]
42. Hou J, Tan G, Fink GR, Andrews BJ, Boone C, Complex modifier landscape underlying genetic background effects. Proc Natl Acad Sci U S A 116, 5045 (2019). [PubMed: 30804202]
43. Mullis MN, Matsui T, Schell R, Foree R, Ehrenreich IM, The complex underpinnings of genetic background effects. Nat Commun 9, 3548 (2018). [PubMed: 30224702]
44. Schell R, Mullis MN, Matsui T, Foree R, Ehrenreich IM, Genetic architecture of a mutation's expressivity and penetrance. bioRxiv, 2020.04.03.024547 (2020).
45. Bloom JS et al. , Genetic interactions contribute less than additive effects to quantitative trait variation in yeast. Nat Commun 6, 8712 (2015). [PubMed: 26537231]
46. Huang W, Mackay TF, The Genetic Architecture of Quantitative Traits Cannot Be Inferred from Variance Component Analysis. PLoS Genet 12, e1006421 (2016). [PubMed: 27812106]
47. Fang G et al. , Discovering genetic interactions bridging pathways in genome-wide association studies. Nat Commun 10, 4274 (2019). [PubMed: 31537791]
48. Wang W et al. , Pathway-based discovery of genetic interactions in breast cancer. PLoS Genet 13, e1006973 (2017). [PubMed: 28957314]
49. Ghandi M et al. , Next-generation characterization of the Cancer Cell Line Encyclopedia. Nature 569, 503 (2019). [PubMed: 31068700]
50. Meyers RM et al. , Computational correction of copy number effect improves specificity of CRISPR-Cas9 essentiality screens in cancer cells. Nat Genet 49, 1779 (2017). [PubMed: 29083409]
51. Tsherniak A et al. , Defining a Cancer Dependency Map. Cell 170, 564 (2017). [PubMed: 28753430]
52. Deshpande R et al. , Efficient strategies for screening large-scale genetic interaction networks. bioRxiv, (2017).
53. Kuzmin E et al. , Synthetic genetic array analysis for global mapping of genetic networks in yeast. Methods Mol Biol 1205, 143 (2014). [PubMed: 25213244]
54. Baryshnikova A et al. , Quantitative analysis of fitness and genetic interactions in yeast on a genome scale. Nature methods 7, 1017 (2010). [PubMed: 21076421]
55. Baryshnikova A, Systematic Functional Annotation and Visualization of Biological Networks. Cell Syst 2, 412 (2016). [PubMed: 27237738]
56. Myers CL, Barrett DR, Hibbs MA, Huttenhower C, Troyanskaya OG, Finding function: evaluation methods for functional genomic data. BMC Genomics 7, 187 (2006). [PubMed: 16869964]
57. Kofoed M et al. , An Updated Collection of Sequence Barcoded Temperature-Sensitive Alleles of Yeast Essential Genes. G3 (Bethesda) 5, 1879 (2015). [PubMed: 26175450]
58. Subramanian A et al. , Gene set enrichment analysis: a knowledge-based approach for interpreting genome-wide expression profiles. Proc Natl Acad Sci U S A 102, 15545 (2005). [PubMed: 16199517]
59. Korotkevich G, Sukhov V, Sergushichev A, Fast gene set enrichment analysis. bioRxiv, 060012 (2019).
60. Usaj M et al. , TheCellMap.org: A Web-Accessible Database for Visualizing and Mining the Global Yeast Genetic Interaction Network. G3 (Bethesda) 7, 1539 (2017). [PubMed: 28325812]

61. Hoose SA et al. , A systematic analysis of cell cycle regulators in yeast reveals that most factors act independently of cell size to control initiation of division. PLoS Genet 8, e1002590 (2012). [PubMed: 22438835]

62. Giaever G et al. , Functional profiling of the Saccharomyces cerevisiae genome. Nature 418, 387 (2002). [PubMed: 12140549]

63. Meldal BHM et al. , Complex Portal 2018: extended content and enhanced visualization tools for macromolecular complexes. Nucleic Acids Res 47, D550 (2019). [PubMed: 30357405]

64. Cherry JM et al. , Saccharomyces Genome Database: the genomics resource of budding yeast. Nucleic Acids Res 40, D700 (2012). [PubMed: 22110037]

65. Krogan NJ et al. , Global landscape of protein complexes in the yeast Saccharomyces cerevisiae. Nature 440, 637 (2006). [PubMed: 16554755]

66. Gavin AC et al. , Proteome survey reveals modularity of the yeast cell machinery. Nature 440, 631 (2006). [PubMed: 16429126]

67. Tarassov K et al. , An in vivo map of the yeast protein interactome. Science 320, 1465 (2008). [PubMed: 18467557]

68. Babu M et al. , Interaction landscape of membrane-protein complexes in Saccharomyces cerevisiae. Nature 489, 585 (2012). [PubMed: 22940862]

69. Koch EN et al. , Conserved rules govern genetic interaction degree across species. Genome biology 13, R57 (2012). [PubMed: 22747640]

70. Huttenhower C, Hibbs M, Myers C, Troyanskaya OG, A scalable method for integration and functional analysis of multiple microarray datasets. Bioinformatics 22, 2890 (2006). [PubMed: 17005538]

71. Stark C et al. , The BioGRID Interaction Database: 2011 update. Nucleic Acids Res 39, D698 (2011). [PubMed: 21071413]

72. Yu H et al. , High-quality binary protein interaction map of the yeast interactome network. Science 322, 104 (2008). [PubMed: 18719252]

73. Huh WK et al. , Global analysis of protein localization in budding yeast. Nature 425, 686 (2003). [PubMed: 14562095]

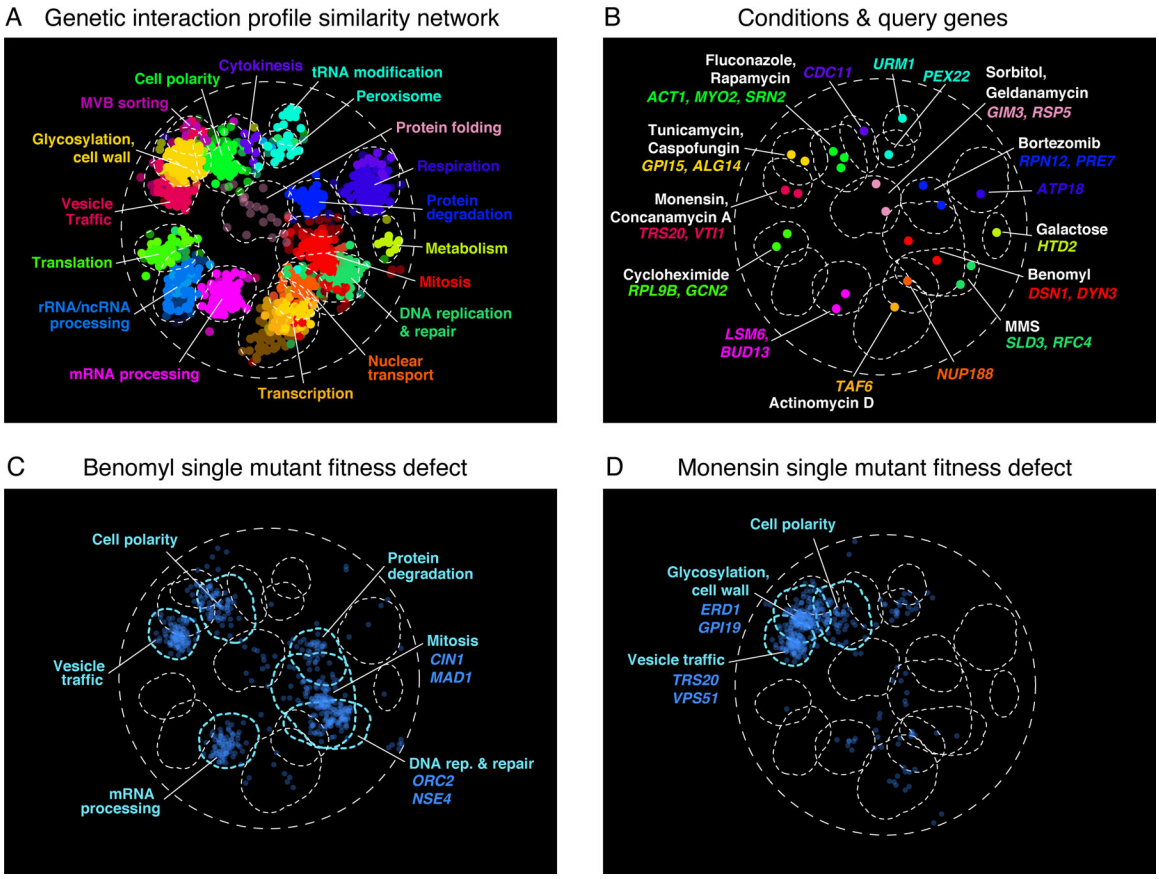

Figure 1. A differential single mutant fitness catalog.

(A) A global genetic profile similarity network encompassing most nonessential and essential yeast genes(11). The similarity network was annotated using Spatial Analysis of Functional Enrichment (SAFE) (55), identifying network regions enriched for similar GO biological process terms, which are color-coded. (B) Conditions and query genes selected for this study. Location of each query gene on the global genetic interaction profile similarity network is indicated. Bioprocesses targeted by selected bioactive compounds are also shown. (C) Regions of the global similarity network significantly enriched for genes exhibiting differential single mutant fitness defects in Benomyl. (D) Regions of the global similarity network significantly enriched for genes exhibiting differential single mutant fitness defects in Monensin. For both (C) and (D), regions of the global similarity network significantly enriched for genes exhibiting negative differential fitness defects were mapped using SAFE. Examples of genes located in the most enriched regions are indicated in blue.

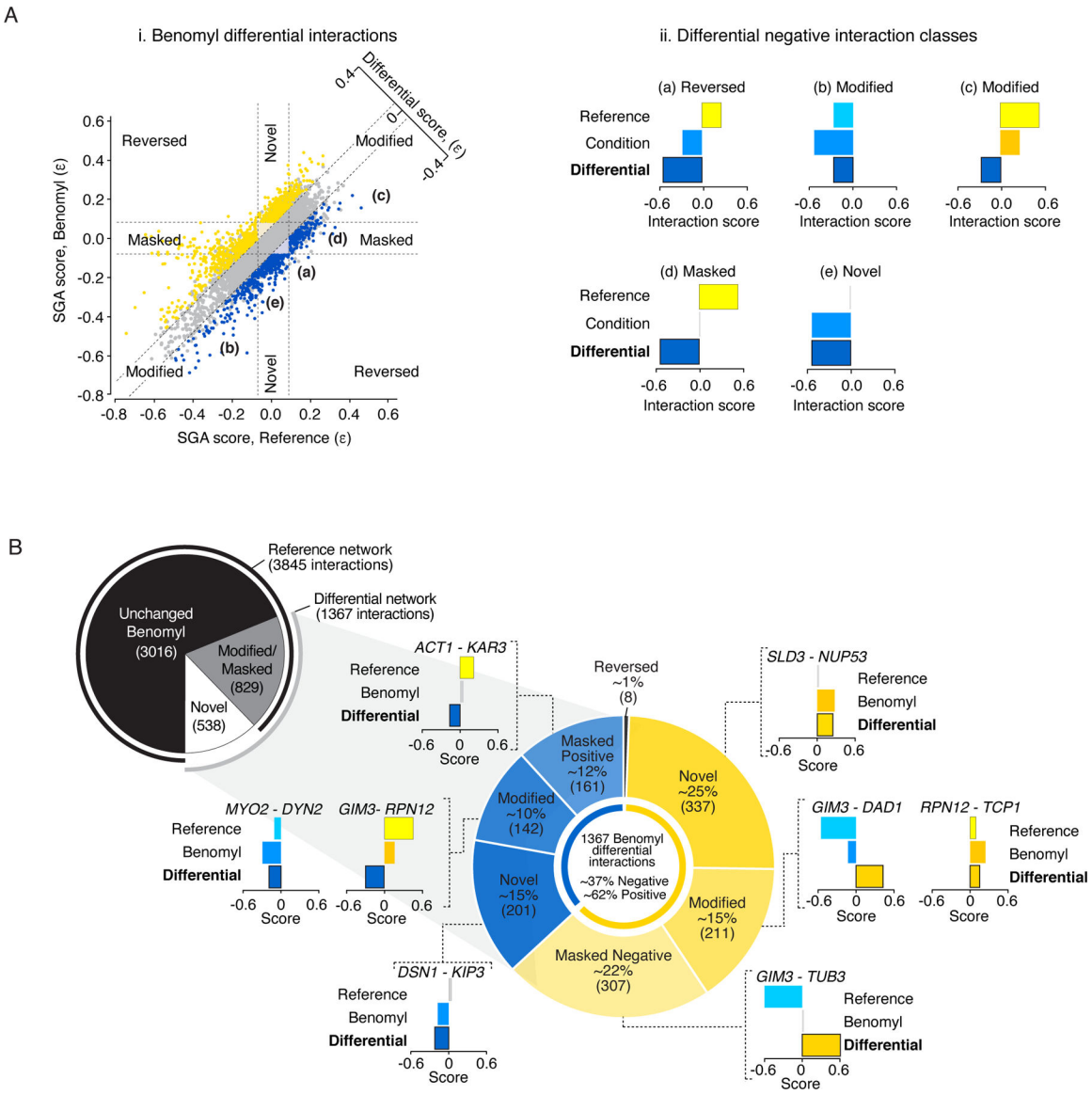

Figure 2. Classification of differential interactions.

(A) (i) Scatter plot of genetic interaction scores between the reference condition (x-axis) and Benomyl-treated screens (y-axis). Gene pairs with significant differential negative (blue) or differential positive (yellow) interactions are indicated. Schematic examples of differential negative interactions from each class are indicated by a letter (a-e) on the scatter plot are shown in (ii); (ii) Schematic illustration of different classes of differential negative interactions. Specific classes of differential negative interactions are indicated and colored in shades of blue. Specific classes of differential positive interactions are indicated and colored in shades of yellow. (B) The number of genetic and differential interactions identified from SGA screens performed in Benomyl and in the reference condition. The fraction of significant reference condition genetic interactions that do not exhibit a significant differential interaction are shown in black. The fraction of differential interactions is shown in grey and white. The outer black and grey rings indicate the size of the reference

and differential interaction networks mapped in the reference and Benomyl conditions, respectively (inset). The larger chart summarizes the total number of negative and positive Benomyl differential genetic interactions identified at an intermediate score threshold. The fraction of negative and positive interactions classified as reversed, novel, modified or masked is indicated. Specific classes of differential negative interactions are indicated and colored in shades of blue. Specific classes of differential positive interactions are indicated and colored in shades of yellow. Examples of gene pairs in each interaction subclass along with their corresponding reference, condition and differential genetic interaction scores are shown.

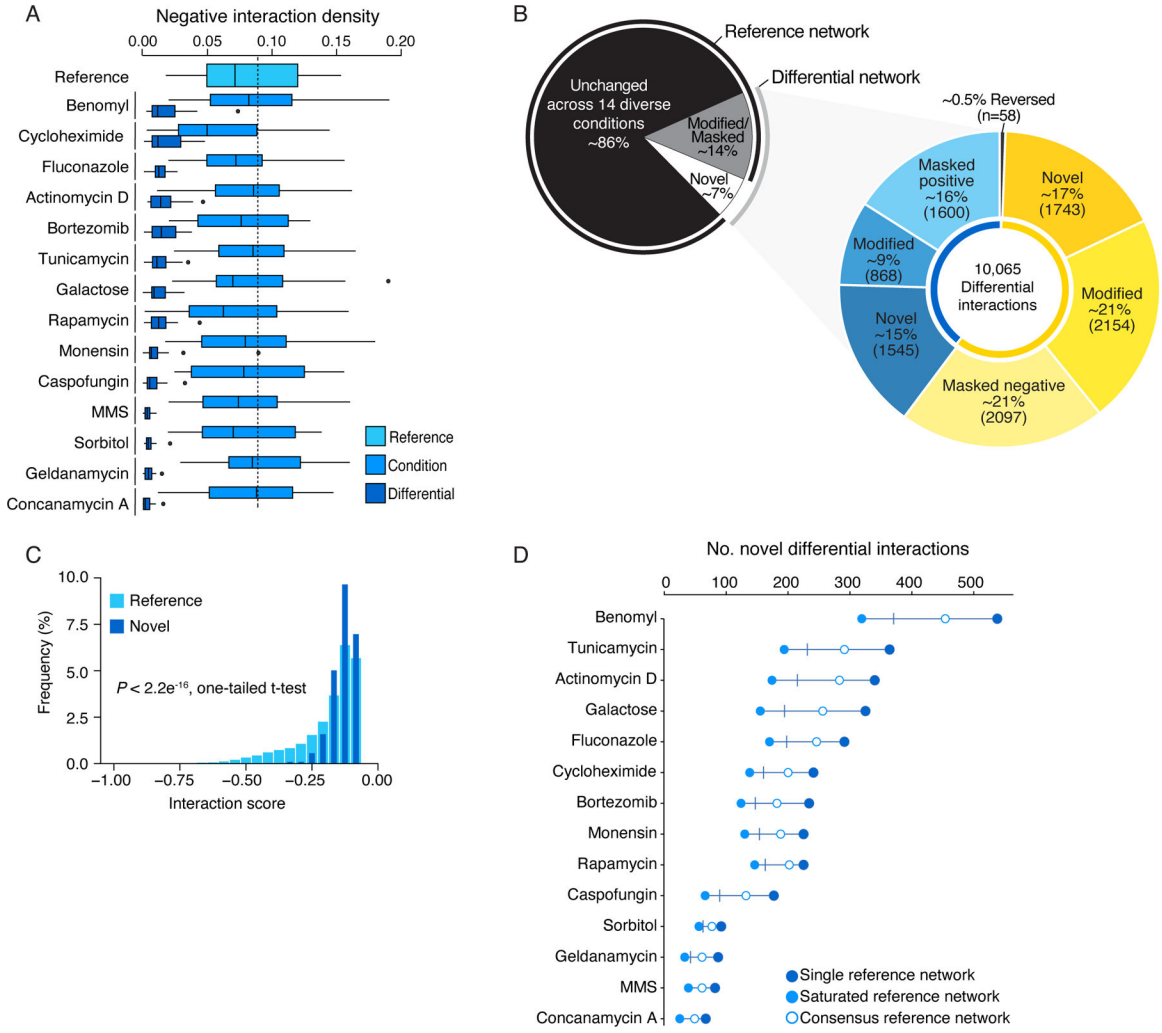

Figure 3. The relative contribution of reference genetic interactions and differential interactions to the yeast genetic network.

(A) Box plots showing the distribution of negative genetic and differential negative interaction density (total number of interactions/total gene pairs tested) per condition and per query mutant screened. The dotted line indicates the average genetic interaction density for the same set of array genes in the global genetic interaction network (11). (B) The average fraction of genetic and differential interactions identified from SGA screens performed in the reference and one additional condition. The fraction of significant reference condition genetic interactions that do not exhibit a significant differential interaction are shown in black. Modified and masked differential interactions, which overlap with interactions identified in the reference condition, and novel differential interactions are indicated. The outer black and grey rings indicate the average size of the reference and differential interaction networks mapped for one additional condition, respectively. The colored diagram summarizes the total number of negative and positive differential genetic interactions identified at an intermediate score threshold from analysis of 14 different test conditions. The fraction of negative (shades of blue) and positive (shades of yellow) interactions classified as reversed, novel, modified or masked is indicated. (C) Distribution of negative

genetic interaction scores (light blue) and novel differential negative interaction scores (dark blue). (D) The number of novel differential interactions identified per condition using different reference genetic interaction networks. Reference networks were defined by exhaustively sampling all possible combinations from 1 to 14 biological replicate screens. The maximum number of novel differential interactions based on comparison to a single matched reference network for each condition is shown in dark blue. The minimum number of novel differential interactions based on comparison to a saturated reference network that combines all 14 replicates (union) is shown in light blue. The number of novel interactions based on comparison to a consensus MCMC-derived reference network (23) is also indicated (open circles). Vertical bars indicate the median number of novel differential interactions across all possible reference network combinations.

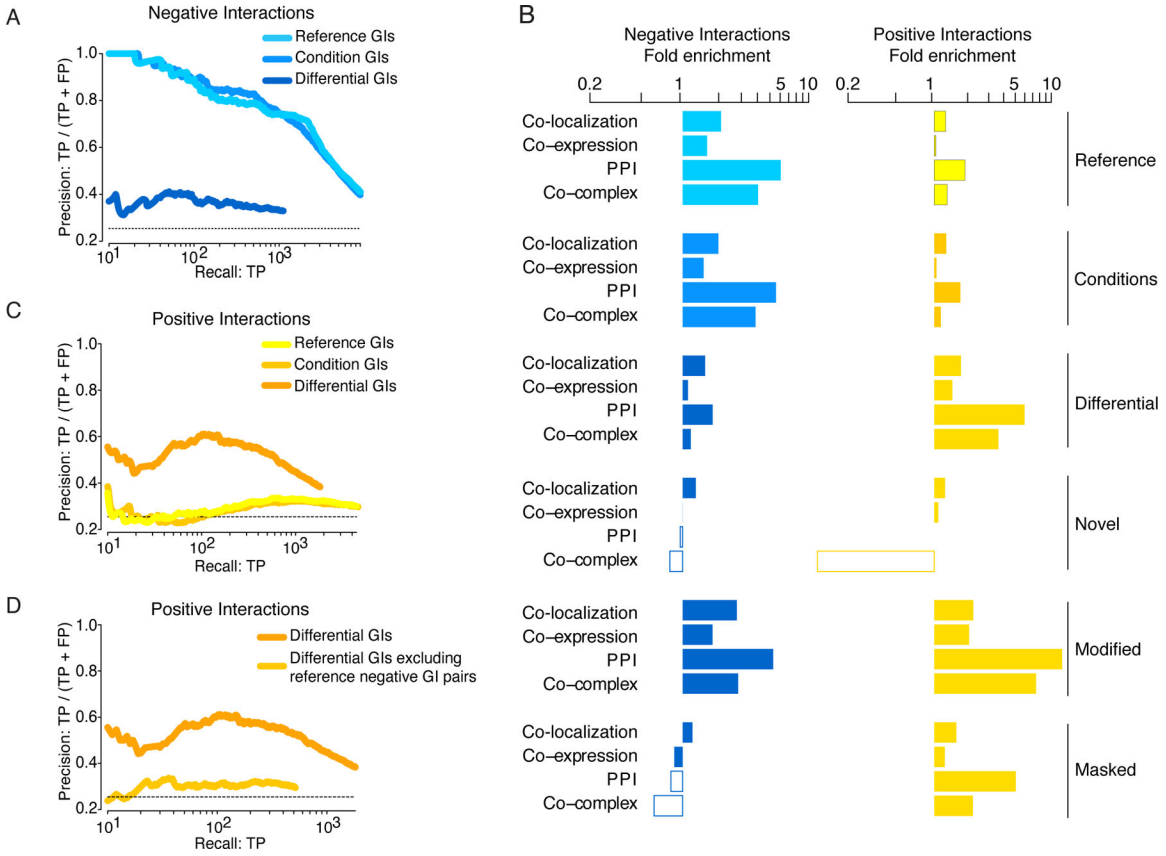

Figure 4. Functional evaluation of differential interactions.

(A) Plots of precision versus recall (number of true positives (TP)) for negative genetic and differential interactions, as determined by our genetic interaction score (|ε| >0.08, $P < 0.05$). True positive interactions were defined as those involving gene pairs co-annotated to a gold standard set of GO terms, as defined elsewhere (56). The background precision at which true positives are randomly identified is indicated by the dotted line. The precision and recall values were calculated as previously described (19). (B) Fold enrichment for negative (blue) and positive (yellow) genetic and differential interactions among co-localized, co-expressed, physically interacting, or co-complexed gene pairs or their encoded proteins were calculated for genetic interactions identified in the reference condition, 14 conditions and each differential interaction class. Comparisons based on fewer than 10 overlapping gene pairs are indicated (open boxes). (C-D) Plots of precision versus recall (number of true positives (TP)) for positive genetic and differential interactions, as determined by our genetic interaction score (|ε| >0.08, $P < 0.05$). True positive interactions were defined as those involving gene pairs co-annotated to a gold standard set of GO terms, as defined elsewhere (56). The background precision at which true positives are randomly identified is indicated by the dotted line. The precision and recall values were calculated as described (19).

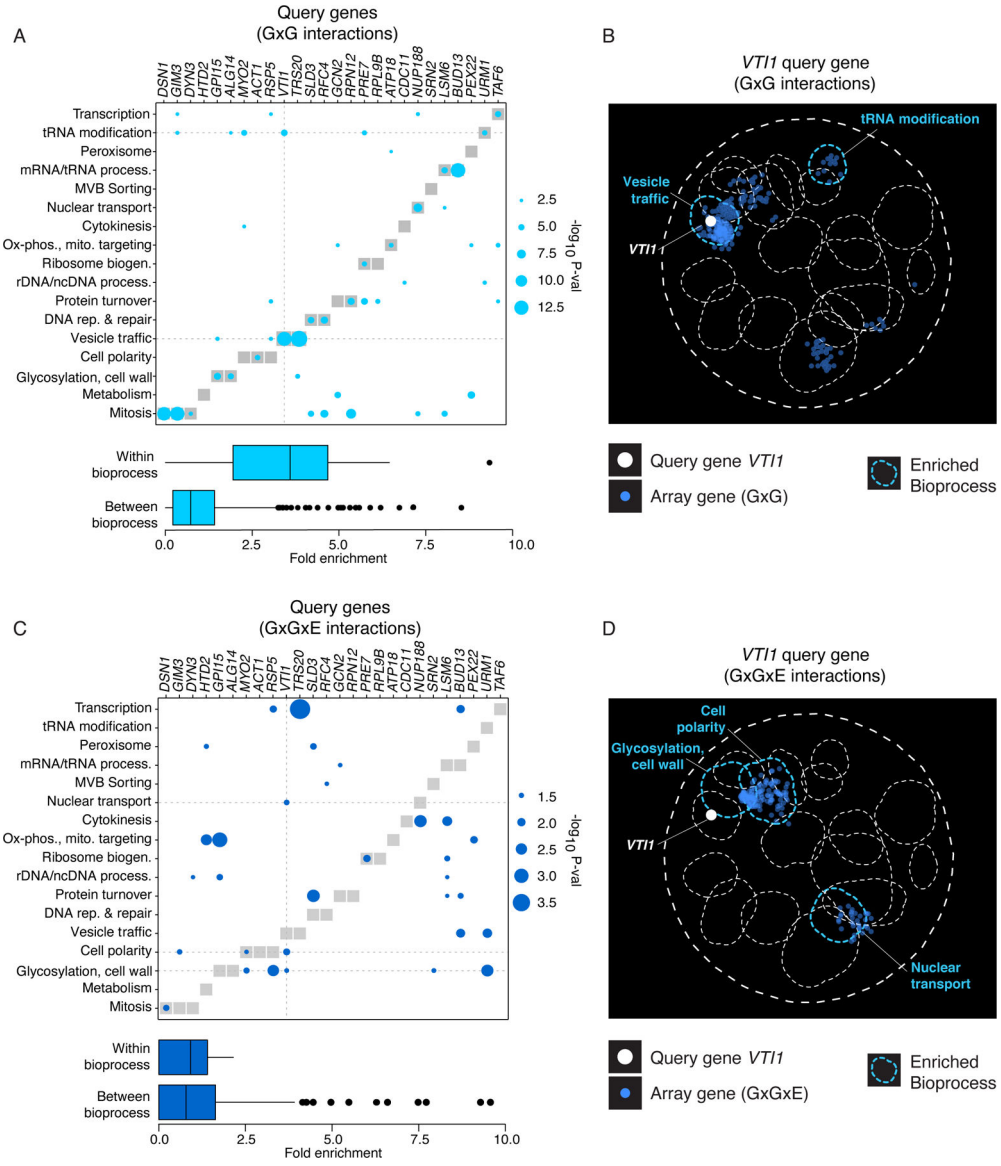

Figure 5. Functional distribution of query gene negative genetic and novel differential negative interactions.

(A) Negative genetic interactions for each query gene (x-axis) in the reference condition were tested for enrichment for array genes in each of the biological processes indicated (y-axis). Node size reflects the statistical significance of enrichment and the shade boxes along the diagonal highlight instances where the query and array genes belong to the same biological process cluster on the global genetic interaction profile similarity network (11). Dotted lines indicate bioprocesses enriched for negative genetic interactions with the *VTI1* query gene. The average fold enrichment of negative genetic interactions within and between specific biological processes is shown in the box plot. (B) Regions of the global genetic interaction profile similarity network significantly enriched for array genes exhibiting negative genetic interactions with the *VTI1* query gene in the reference condition were mapped using Spatial analysis of functional enrichment (SAFE)(55). The functional regions of the global similarity network significantly enriched for interactions with *VTI1*

are indicated by blue dotted lines. Array genes enriched for negative genetic interactions are shown in blue. The location of the *VTI1* query gene on the global similarity network is indicated by a white node. (C) Novel differential negative interactions for each query gene (x-axis) across all 14 test conditions were tested for enrichment for array genes in each of the biological processes (y-axis). Node size reflects the statistical significance of enrichment and the shade boxes along the diagonal highlight instances where the query and array genes would have belonged to the same biological process cluster on the global genetic interaction profile similarity network (11). Dotted lines indicate bioprocesses enriched for novel differential negative interactions with the *VTI1* query gene. The average fold enrichment of novel differential negative interactions within and between specific biological processes is shown in the box plot. (D) Regions of the global genetic interaction profile similarity network significantly enriched for array genes exhibiting novel differential negative interactions with the *VTI1* query gene were mapped using SAFE (55). The functional regions of the global similarity network significantly enriched for interactions with *VTI1* are indicated by blue dotted lines. Array genes enriched for novel differential negative interactions are shown in blue. The location of the *VTI1* query gene on the global similarity network is indicated by a white node.

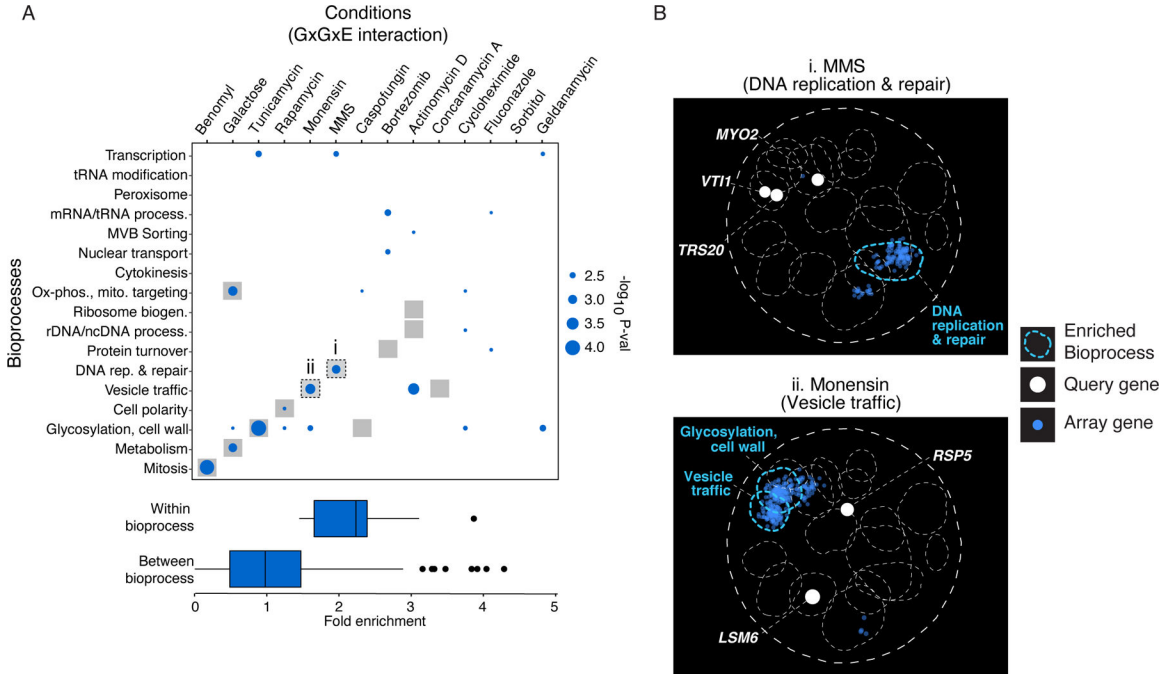

Figure 6. Functional distribution of novel differential negative interactions across conditions.

(A) Novel differential negative interactions from each of the 14 conditions (x-axis), were tested for enrichment for array genes grouped according to the biological processes indicated (y-axis). Node size reflects the statistical significance of enrichment and the shaded boxes along the diagonal indicate the biological process targeted by a particular condition. The average fold enrichment of novel negative interactions within biological processes targeted by a specific condition and interactions enriched within biological processes unrelated to the condition are shown in the box plot. (B) Regions of the global similarity network significantly enriched for array genes exhibiting novel negative differential interactions in (i) MMS or (ii) Monensin were mapped using SAFE (55). The functional region of the global similarity network targeted by Monensin and MMS are indicated by blue dotted lines. Array genes enriched for novel differential negative interactions are shown in blue. Query gene(s) responsible for enrichment of novel differential interactions with the indicated array genes are shown as white nodes.

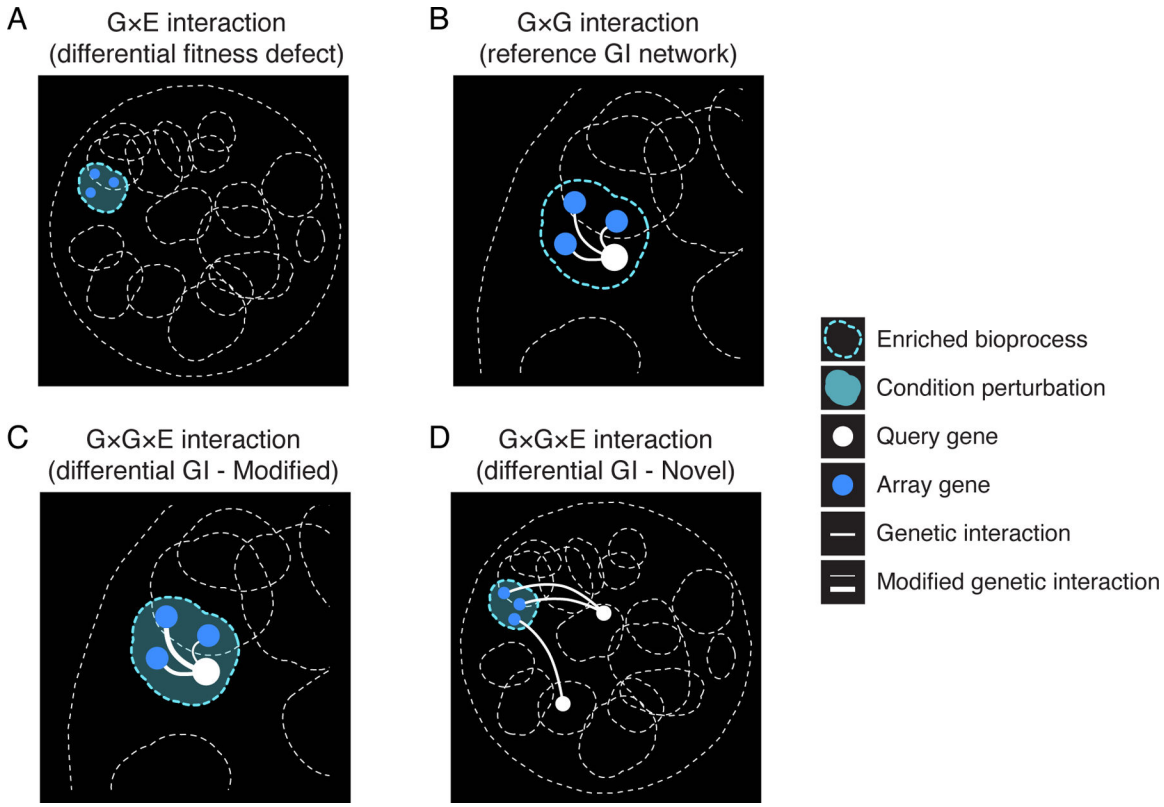

Figure 7. Schematic summary of functional connections mediated by gene-environment (GxE), gene-gene (GxG) and gene-gene-environment (GxGxE) interactions.

(A) GxE interactions. Genes will roles in the same bioprocess (illustrated by dotted outlines) are often sensitive to an environmental perturbation affecting that process (blue nodes – array genes; shaded blue area – condition perturbation). (B) GxG interactions. Genetic interactions (white edges) tend to connect array and query genes (white nodes) functioning in the same bioprocess. (C) GxGxE interactions (modified). Many genetic interactions are modulated by the environment (white edges) creating a modified differential genetic interaction that varies in magnitude when compared to the equivalent genetic interaction on the reference network. Modified GxGxE interactions often connect functionally related query-array gene pairs. (D) GxGxE interactions (novel). Novel GIs, which were not detected in the reference condition, often connect genes involved in a bioprocess perturbed by a specific condition to distant, functionally unrelated genes.